PLOS CLIMATE

RESEARCH ARTICLE

Effect of urban heat island mitigation strategies on precipitation and temperature in Montreal, Canada: Case studies

Audrey Lauer[1]*, **Francesco S. R. Pausata**[1], **Sylvie Leroyer**[2], **Daniel Argueso**[3]

1 Department of Earth and Atmospheric Sciences, University of Quebec in Montreal, Montreal, Quebec, Canada, **2** Meteorological Research Division, Environment and Climate Change Canada, Dorval, Quebec, Canada, **3** Physics Department, University of the Balearic Islands, Palma, Spain

* lauer.audrey@courrier.uqam.ca

OPEN ACCESS

Citation: Lauer A, Pausata FSR, Leroyer S, Argueso D (2023) Effect of urban heat island mitigation strategies on precipitation and temperature in Montreal, Canada: Case studies. PLOS Clim 2(6): e0000196. https://doi.org/10.1371/journal.pclm.0000196

Editor: Rohinton Emmanuel, Glasgow Caledonian University, UNITED KINGDOM

Received: November 29, 2022

Accepted: May 7, 2023

Published: June 26, 2023

Data Availability Statement: All data is available freely under the DOI: 10.5281/zenodo.7738807 Direct link to the data: https://doi.org/10.5281/zenodo.7738807.

Funding: This work was supported by the MCIN/AEI (PID2019-105253RJ-I00 project direct costs financed by MCIN/AEI/10.13039/501100011033 to DA) The funders had no role in study design, data collection and analysis, decision to publish, or preparation of the manuscript. All the numerical simulations in this study were performed on the

Abstract

High-resolution numerical weather prediction experiments using the Global Environmental Multiscale (GEM) model at a 250-m horizontal resolution are used to investigate the effect of the urban land-use on 2-m surface air temperature, thermal comfort, and rainfall over the Montreal (Canada) area. We focus on two different events of high temperatures lasting 2–3 days followed by intense rainfall: one is a large-scale synoptic system that crosses Montreal at night and the other is an afternoon squall line. Our model shows an overall good performance in adequately capturing the surface air temperature, dew-point temperature and rainfall during the events, although the precipitation pattern seems to be slightly blocked upwind of the city. Sensitivity experiments with different land use scenarios were conducted. Replacing all urban surfaces by low vegetation showed an increase of human comfort, lowering the heat index during the night between 2˚ and 6˚C. Increasing the albedo of urban surfaces led to an improvement of comfort of up to 1˚C during daytime, whereas adding street-level low vegetation had an improvement of comfort throughout the day of up to 0.5˚C in the downtown area. With respect to precipitation, significant differences are only seen for the squall line event, for which removing the city modifies the precipitation pattern. For the large-scale synoptic system, the presence of the city does not seem to impact precipitation. These findings offer insight on the effects of urban morphology on the near-surface atmospheric conditions.

1 Introduction

Cities occupy a small fraction of the Earth's surface, yet over half of the world's population lives in urban areas, a number that will significantly increase in the next decades [1]. Cities modify the local environment because they are built with materials and geometries that clearly differ from the natural landscape. Built structures have an impact on the local climate because they alter surface exchanges of heat, moisture, momentum, and radiation with the atmosphere. A complete understanding of these effects is crucial to identify and reduce the risks that urban dwellers are exposed to.

supercomputer facilities at Environment and Climate Change Canada.

Competing interests: The authors have declared that no competing interests exist.

Initially observed and documented in the 1800s, urban areas are warmer relative to their rural surroundings [2]. This phenomenon is referred to as the canopy urban hat island (UHI) and processes explaining the unique local climate of cities have been well documented [3,4]. Materials used in cities have low reflectance, are good thermal conductors and have greater heat storage capacity, so they are more efficient than the natural materials at absorbing atmospheric radiation fluxes and heat, which is then released at night mainly through sensible heat flux. Urban surfaces are mostly impervious, which alters the water budget by reducing infiltration and evaporation, and by increasing surface runoff. As a result, there is little water available for evaporative cooling and most turbulent heat exchanges are channelled through sensible heat fluxes. In addition, city landscapes are often less vegetated than rural areas, reducing evapotranspiration from plants and its effect on temperature. Urban geometry accentuates these effects by trapping energy because solar radiation is reflected multiple times by urban surfaces and thus the probability for it to be absorbed by the city fabric is larger [5]. Urban areas reduce the wind, which enhances the heat trapping in the city [5,6]. Anthropogenic heat sources (i.e. road traffic, industry, heating and air-conditioning) and atmospheric pollution also contribute to increasing the intensity of the urban heat island [5].

Urban planners tend to adopt many different strategies to reduce the strength of the UHI and its potential effects on the increasing urban population. Common mitigation strategies are, for example, adding green infrastructures such as green roofs, parks and trees [7–10], and increasing the reflectivity of urban surfaces [10–14]. Replacing urban surfaces with vegetation lowers air temperature due to increased evapotranspiration and less surface warming during the day. Furthermore, low vegetation might enhance heat release at night since it often has a high sky-view factor. On the other hand, vegetation also adds water vapor to the air, potentially decreasing human comfort on local population. Studies show that in general heat stress is typically lowered when vegetation is added [8,15], which is beneficial to urban population. The type of vegetation (i.e. low or high vegetation) added and its placement inside the urban canyon can have a different effect on thermal comfort, for example, trees offer shade and interact with radiation and are more effective than grass in improving comfort [7]. Increasing urban surface albedo decreases daytime air temperature due to higher reflection of solar radiation that causes less surface warming. Nighttime impacts of albedo change seem instead to be negligible [10,11,14]. For this mitigation strategy, the impact on human comfort can vary depending on the way it is assessed. Recent studies have shown that increasing the ground-level albedo may well decrease pedestrian comfort due to increased reflection [14,16,17]. The effectiveness of these strategies is also greatly affected by the geographical location, size, and composition of the city.

In the last decade, it has also been shown that urban areas can have a sizeable impact on precipitation. Observational and modeling studies in mostly North American and Asian megacities reviewed by Liu & Niyogi show a rainfall enhancement of 16% over and 18% downwind of the city (20–50 km from the city center) [18]. Our understanding on the urban processes that modify rainfall is still evolving because precipitation is influenced by many factors from large-scale synoptic systems to local cloud microphysics. The main mechanisms through which urban areas can influence precipitation are the following, in no particular order of importance:

- An increase in low-level convergence due to increased roughness of cities which impacts convection over the urban areas [19];
- Higher temperatures over cities due to the UHI tend to destabilize atmosphere, therefore create UHI-generated convective clouds [5,20,21];

- Enhanced concentration of atmospheric aerosols over cities due to pollution are sources of cloud condensation nuclei (CCN) and influence the radiative transfer between the cloud layer and the surface. These effects are summarized in [22];
- Storms tend to either bifurcate around cities [19] or split into small convective cells upwind from the city [23].

These processes are not always represented correctly in numerical studies, thus could explain the differences with observational studies reported in [18]. Nevertheless, numerical experiments have become more and more important to understand interactions between the cities and the atmosphere as different urban processes can be isolated to disentangle their relative impact on local climate.

In this study, numerical weather prediction (NWP) case studies in the Montreal (Canada) region are explored. During summertime, important UHI both night and daytime can be observed in Montreal. While the impact of this city on temperature and heat stress has been previously investigated [24,25], few studies have hitherto explored the impact of Montreal UHI on summertime precipitation. Located in the Saint-Laurence River, Montreal has been affected by significant flooding events. For example, springtime flooding in the Great Montreal region is typically linked to rainfall associated with extended thaw periods, hence leading to rapid melting of winter snowpack [26]. In July 1987, a series of strong thunderstorms that crossed the island in the afternoon generated significant downpours, which paralyzed the city. This event followed a significant heat wave over the region, which likely intensified the storm. Since previous studies have shown an enhancement of rainfall over urban areas and given that urbanized areas are growing, flooding events are more likely to occur in the future [27]. Moreover, impervious surfaces in cities intensify surface runoff and reduces water infiltration, which increases the flooding frequency [28]. Additional factors beyond the urban environment may produce an intensification of extreme events, for instance higher temperatures due to climate change increases the atmosphere's water-holding capacity [29]. Studies have indeed shown a higher number of flooding events due to increasing urbanization and climate change [28,30,31], which urges cities to adapt.

The main objectives of this paper are, to understand how the urban environment of Montreal influences local temperature and human comfort during heat waves and to evaluate the impact of the city on rainfall following these heat waves. To achieve this, two heat events immediately followed by intense precipitation are studied using a high-resolution numerical model. Furthermore, different mitigation scenarios replicating urban design strategies are investigated to assess their effectiveness on improving comfort. The manuscript is divided as follows: section 2 presents the models used and the experimental design; section 3 shows the results from two different case studies; section 4 summarizes and discusses the key findings of this study.

2 Methodology

2.1 NWP models and system

The NWP experiments are conducted at a 250-m horizontal grid spacing. They are obtained through a nesting technique starting from the 2.5-km operational forecasts from Environment and Climate Change Canada (ECCC) High-Resolution Deterministic Prediction System (HRDPS) and dynamically downscaled to a 1-km and then 250-m resolution. The domains for the HRDPS and experiments at 1 km and 250 m centered on the city of Montreal are shown in the upper panel of Fig 1.

The atmospheric model used in this study is the Global Environmental Multiscale (GEM) model version 5.1 [32,33]. GEM is a non-hydrostatic model on a staggered Arakawa-C

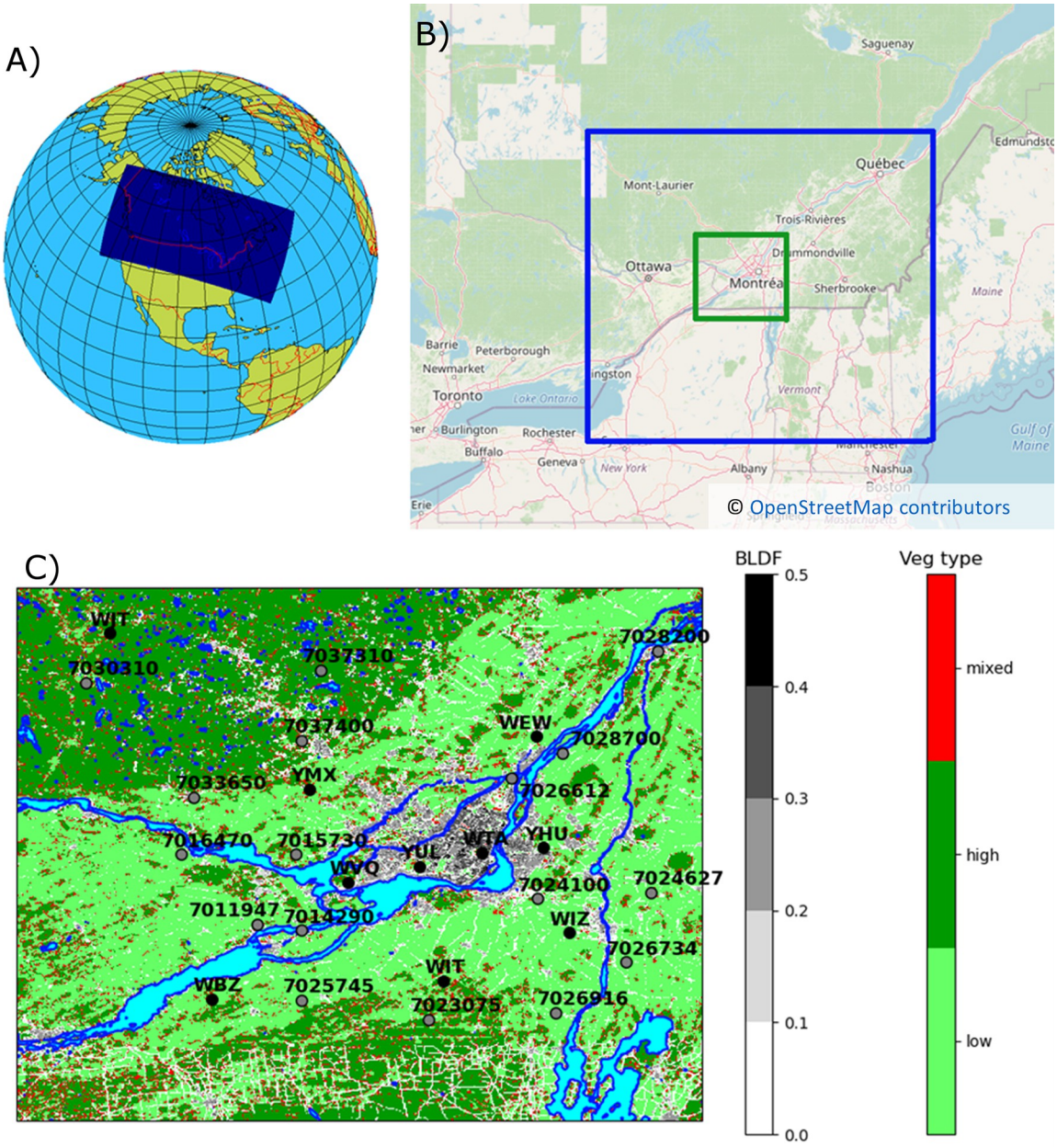

Fig 1. Geographical locations of model domains and weather stations. a) The HDRPS (2.5 km) domain over North America used to drive our model simulations, b) The high-resolution domains at 1km (blue rectangle) and 250m (green rectangle) and c) details of land use on the 250 m grid. The grayscale shows the building fraction, with main roads added in white. The green-red scale shows the main type of vegetation at the grid point. Weather stations are shown (in black: Hourly observations; in grey: Daily observations) with their corresponding national identification (refer to table in the supporting materials for details of stations). Panel b base map is taken from OpenStreetMap, available under the Open Database License (https://www.openstreetmap.org/copyright).

https://doi.org/10.1371/journal.pclm.0000196.g001

horizontal grid and a staggered Charney-Phillips vertical grid. The configuration used in this work is based on a log-hydrostatic-pressure type terrain-following vertical coordinate.

In GEM, surface fluxes are calculated over 5 types of surfaces: natural land, water, glaciers, sea ice and urban. The surface processes over natural land including vegetation in urban areas are represented with the Interaction between Soil-Biosphere-Atmosphere (ISBA) scheme

[34,35]. For built-up surfaces, the surface processes are represented with the Town Energy Balance (TEB) scheme [36,37]. The urban surface uses a canyon representation [38], which is a single road surrounded by buildings (walls and roofs) on each side. Interactions between surfaces such as shadowing and radiation trapping are considered by TEB and three distinct energy budgets are calculated–one for each surface. For water bodies, the surface temperature provided by the operational analysis is considered constant throughout the experiment, given water high heat capacity.

Ancillary data needed as input for TEB are computed directly on the model grid cell based on the methodology of Leroyer et al. (2022) [39] and extended to the entire Canada including Montreal. The most important underlying vectorial dataset are Canvec and Circa-2000 (from Natural Resources Canada) NRCan databases and the Circa-2000 for vegetation and precise building heights and footprints for the downtown area (City of Montreal office). Morphological parameters including aerodynamical roughness are computed at the model grid resolution [40]. Cloud and precipitation processes occurring at sub-grid scales are represented using four different schemes in GEM: a boundary layer clouds scheme, shallow and deep convection schemes and cloud microphysics. In this study, deep convection is considered explicitly resolved because the forecasts are done on a subkilometer grid and therefore the deep convection scheme is not activated. For boundary layer clouds and shallow convection, MoisTKE and Kuo Transient implicit schemes are activated. This configuration is further detailed in [41]. Finally, a two-moment version of the bulk microphysical scheme MY2 is used to represent the grid-scale processes [42].

A similar setup has been used in many studies from ECCC [39,43]. This NWP system down to 250 m grid-spacing is experimental and was built similarly to the NWP system used for the Toronto metropolitan area (Canada) run daily for specific applications. Seasonal objective evaluation revealed a good representation of summertime afternoon convective precipitation [39]. At this scale, part of the turbulence is resolved and the thermal plumes in the mixed boundary-layer–eddies of the size of 1000–1500 m and more might be resolved [44]. The remaining sub-grid scale turbulent component, corresponding to smaller eddies, is computed through a vertical diffusion scheme for which a reduction of the maximum mixing length in neutral conditions from 200 m to 57 m has been applied [45].

2.2 Data for observations and analysis

Data from operational ECCC surface stations is used to evaluate the experiments. Hourly observations for surface variables are available for a few stations in the domain of interest (Fig 1, black dots). These stations are used to validate surface air temperature and humidity, as well as the timing and rainfall rate. More stations are available with daily observations (Fig 1, gray dots), which are used to compare total precipitation accumulations from our experiments. The complete list of stations with their description is available in the supporting materials (S1 Table).

Due to precise representation of the elevation in the model and to moderate slopes in the region, elevation difference between model and in situ stations was found to be less than 10 m and is neglected in this study. In addition, 2-m temperature is computed above the road in the street directly and the reference level is not impacted by the large buildings in downtown.

Another dataset used for validation is the Canadian Precipitation Analysis (CaPA) dataset. The version used in this study is the High-Resolution Deterministic Precipitation Analysis (CaPA-HRDPA), which uses a background field from the HRDPS forecasts and observations from surface stations and radars [46]. 6-h accumulated precipitation at 2.5-km resolution is available for the two studied periods.

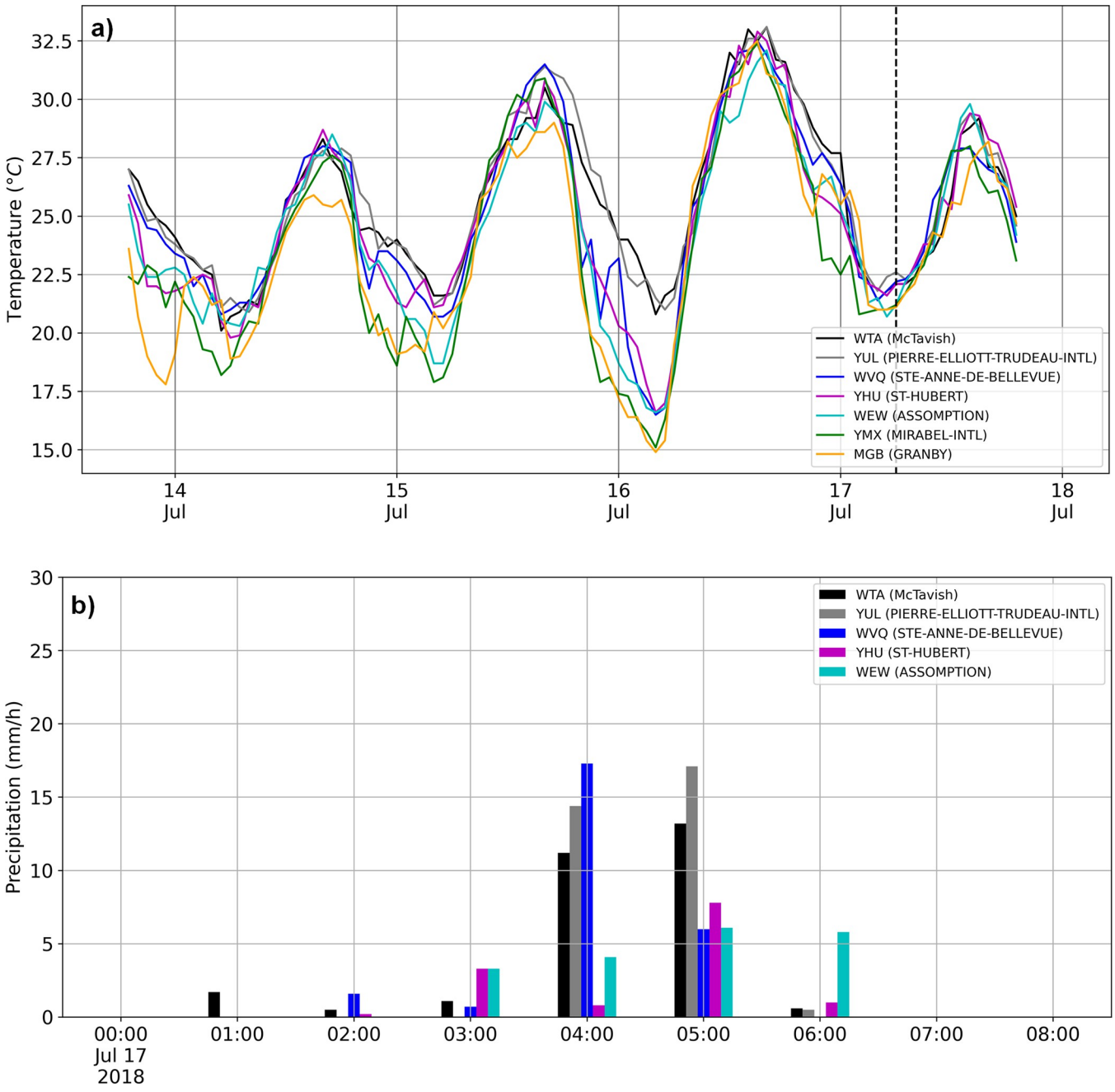

Fig 2. Observed temperature and precipitation for the 2018 event. Observed hourly a) surface air temperature and b) precipitation accumulation at different stations. Precipitation data is missing for Mirabel-Intl and Ste-Anne de Bellevue stations during that period.

https://doi.org/10.1371/journal.pclm.0000196.g002

2.3 Experimental setup

2.3.1 Ensemble setup. In order to account for model internal variability, a 9-member ensemble is formed for each event as sketched in S1 Fig. Each member uses the same driving data from HRDPS forecasts (based on 12 to 24 hours lead-time forecasts), but has a different initialization date, each separated by 12 hours. This is a way for each member to have different initial conditions, and then to evolve in their own way, even with the same boundary

conditions from the HRDPS forecasts. The last initialized member starts at least 12 h before the precipitation event to let the model spin-up. These first forecasted 12 h are not considered in our results analysis.

Initial surface conditions for ISBA are produced from the Canadian Land Data Assimilation System (CaLDAS) downscaled from 2.5 km to 1 km and 250 m and for water bodies from ECCC's analysis. Temperature of the urban surfaces in TEB in contact with the atmosphere is considered the same as the surrounding air temperature at the time of the initialization (surface layer for roads and walls, and first atmospheric level for roofs). Temperature in the deepest layer of road is assumed similar to the soil temperature from ISBA. In addition, a 12-hours spin-up time is considered for the surface temperatures to adjust.

2.3.2 Sensitivity experiments. Four sensitivity experiments are carried out on both the 250-m and 1-km grid for each ensemble member: a control simulation (CTL) using the default land use (as depicted in Fig 1), an experiment without any urban areas (NOURB), a simulation in which the albedo of the urban surfaces is increased (ALB) and another one in which urban vegetation is enhanced (VEG). In the CTL simulation, the urban surface is represented by using a database of rasterized maps of detailed urban and natural classes at a 5-m resolution, following the method used in Leroyer et al. [39] for Toronto. In the NOURB experiment, every urban surface (roads and roofs) is replaced by low vegetation and the TEB scheme is deactivated. In the ALB simulation, the albedo of roads, walls and roofs is modified over 85% of the grid points on the island of Montreal. Road, roof and building wall albedo are increased from 0.20, 0.15 and 0.25 to 0.45, 0.65 and 0.60 respectively. Other city properties (i.e. geometry, composition and materials) are not modified in the ALB experiment.

In VEG, we replace half of the roads on each grid point with low vegetation if the original road fraction is between 0.2 and 0.5. An important thing to note on the operation of the TEB scheme is its separation of urban land use from natural cover. Both are considered completely separated–TEB will calculate variables (i.e. air temperature, humidity and winds) inside the canyon, the ISBA scheme will calculate these variables over vegetation, and weighted average is done for the whole grid point afterwards. To keep the city's geometry fixed, the building aspect ratio is kept the same. In other words, the surface description used by TEB is similar in both VEG and CTL, but the weight attributed to the ISBA scheme's results at the time of the aggregation will be larger.

2.4 Description of the events

This study focuses on two distinct events where surface air temperature values above 30˚C in Montreal were followed by remarkable rainfall.

The first studied period is in July 2018 (Fig 2), when hot days (with temperature values progressively increased up to about 32.5˚C) were followed by a significant rainfall event over the Montreal region associated with a large-scale synoptic system crossing the Montreal Island from the southwest. The event occurred during late night/early morning and brought intense precipitation between 0400 and 0800 local time on the 17th of July 2018 with hourly rainfall amounts reaching about 10–15 mm. A complete analysis of this event will be done in the following sections.

The second studied period is in July 2019, where a series of hot days with temperature reaching up to 30˚C was followed by intense precipitation in the Montreal region. A squall line travelled from the northwest and brought heavy rain and thunderstorms in the region during the late afternoon of the 11th of July 2019 (Fig 3). These systems are typically very unstable and can be further destabilized as cold and humid air travels through hot and dry air over urban areas.

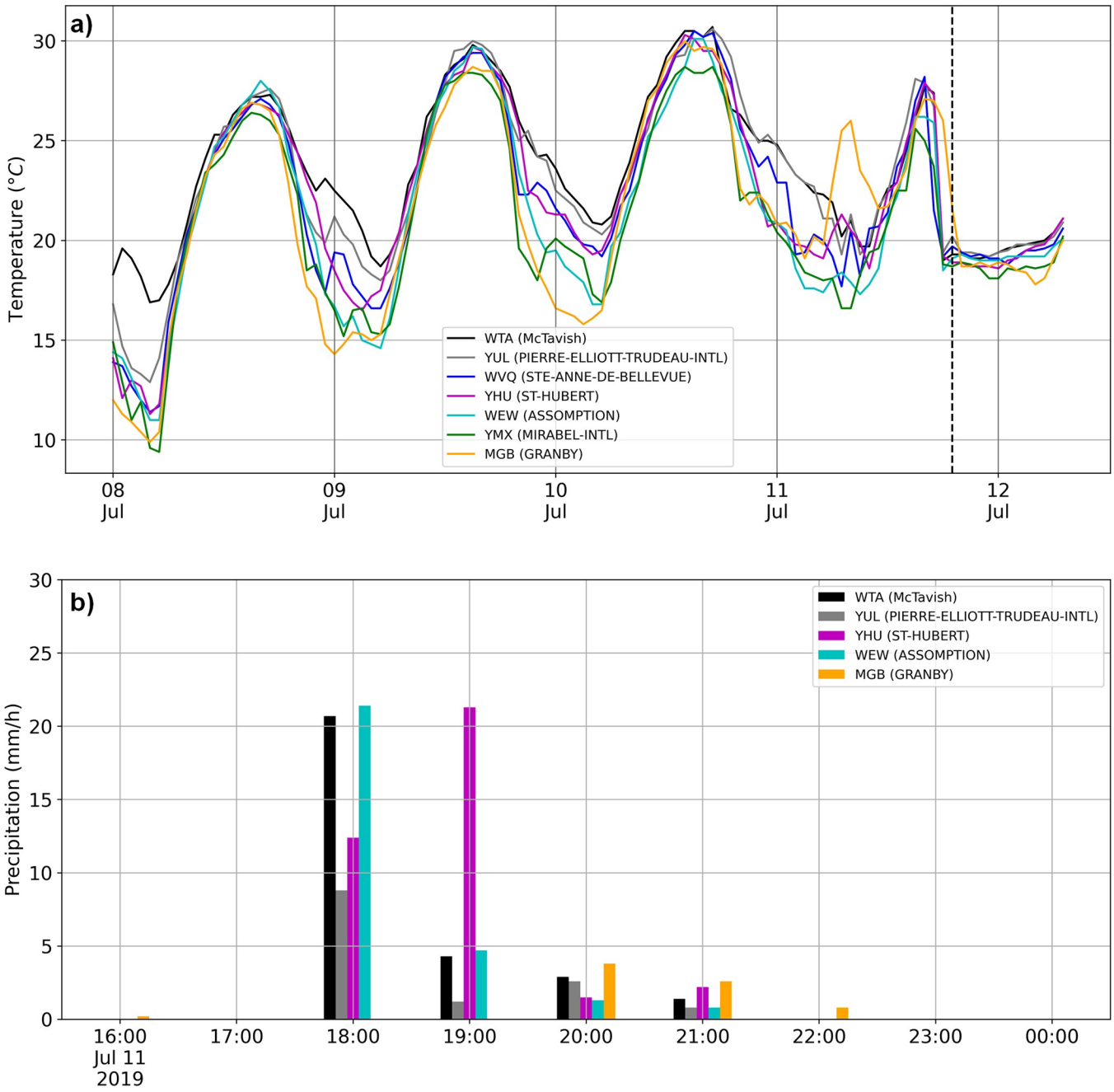

Fig 3. Observed temperature and precipitation for the 2019 event. Same as Fig 2 for July 2019 case study.

https://doi.org/10.1371/journal.pclm.0000196.g003

3 Results

This section is divided in 3 parts. In the first part (Sect. 3.1) we validate the model performance in representing the urban processes and the rainfall events against observations. In Section 3.2 we look at the effects on surface air temperature and humidity of each mitigation scenarios and finally in Section 3.3 we investigate the impacts of NOURB experiment on rainfall relative to the CTL case.

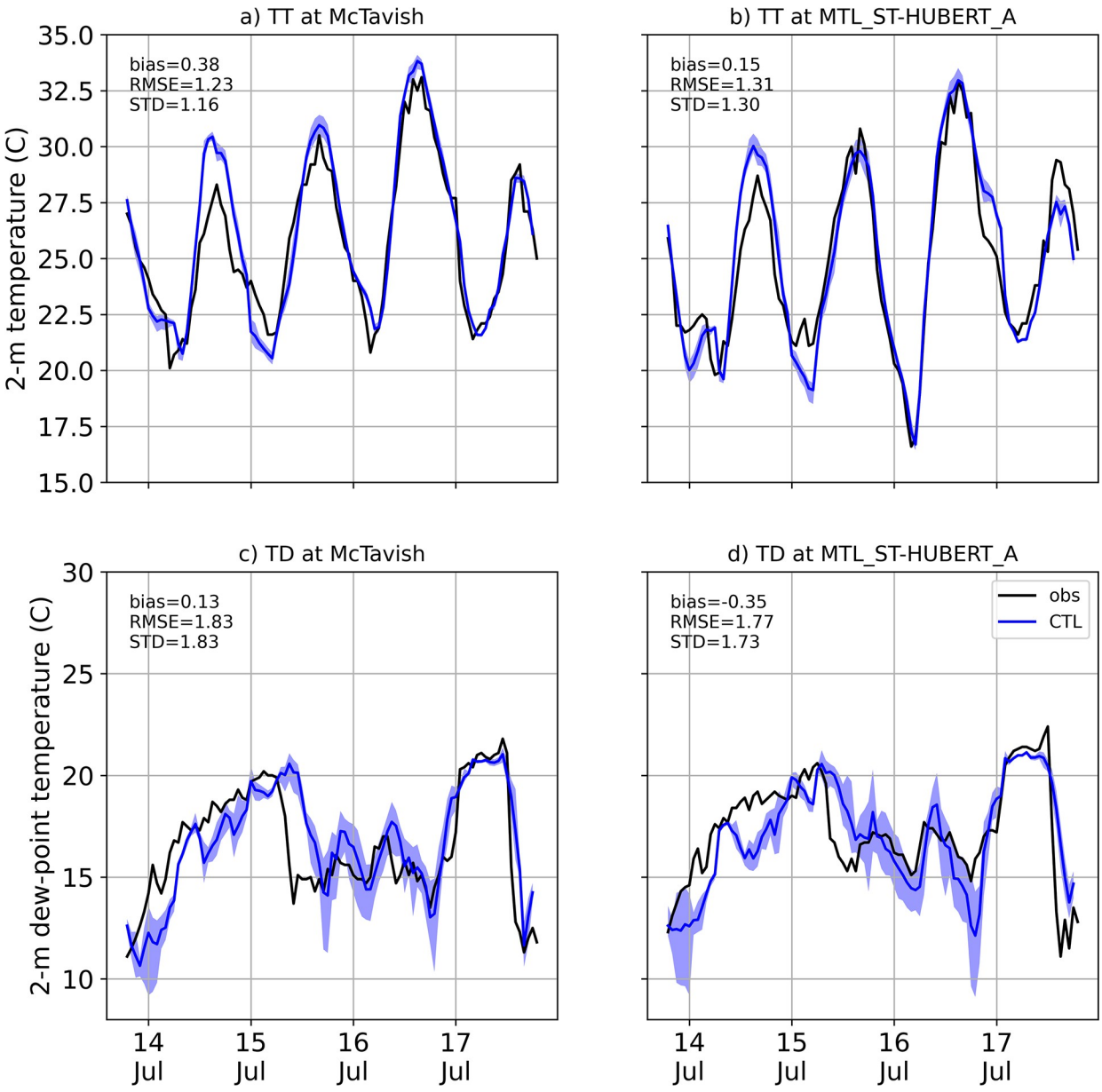

Fig 4. Timeseries of observed and simulated surface variables. Observed (black) and simulated (blue) surface air temperature (TT, a and b) and dew point temperature (TD, c and d) at station McTavish (WTA, a and c) and St-Hubert (YHU, b and d) for the 2018 event. The blue shading shows the ensemble spread.

https://doi.org/10.1371/journal.pclm.0000196.g004

3.1 Control experiment (CTL) versus observations

3.1.1 Surface variables in the CTL experiment. Results for two stations for the July 2018 event are analyzed in this section: McTavish station (WTA) which is in a dense urban area in downtown Montreal, and St-Hubert Airport station (YHU) which is in a suburban area east of Montreal (Fig 1). Other hourly stations analyses are available in the supporting materials.

The model captures well the surface air temperature diurnal cycle during the days prior to the rain event at different locations in the area. Daily maximum temperatures at the urban station (McTavish, Fig 4A) for the 3 days leading to the precipitation event are higher by 1–2˚C in the CTL experiment than the observation. Such discrepancy is likely due to the fact that

measurements are done at a single point, usually over low grass or bare soil [47], whereas the model computes an average over all urban surfaces in a 250-m radius. Hence, in the model the output temperatures also include temperatures over urban surfaces, which are warmer than bare soil and vegetation during the day. At the suburban station (St-Hubert Airport, Fig 4B), maximum temperature is similar in the CTL experiment and the observations. The station is located outside the urban area (Fig 1), where the land use is more uniform (i.e. large fields and roads), thus the conditions experienced by the sensor are more representative of the model grid point average.

At both stations, the temperature from July 14th to the early hours of July 15th of the CTL experiment differs quite substantially from observations. The forecasted daytime surface air temperatures are around 2˚C higher and nighttime temperatures around 1–2˚C cooler than observed temperatures. This indicates a somewhat incorrect model representation of some processes, possibly related to cloud cover or inexact representation of the boundary layer. On the other hand, for the two days leading to the event (July 15th and July 16th) the model correctly captures the surface air temperature diurnal cycle.

Regarding surface dew-point temperature, the results from CTL tend to agree with the available observations but present slight differences (Fig 4C and 4D). In particular, the dew point model behaviour on July 15 and 16th seems delayed by a few hours compared to observations. No delay is simulated in the air temperature, suggesting that the discrepancy in simulating the dew point could be due to a delay in the large-scale moisture advection. During the precipitation events (on July 17th), modelled surface dew point temperature agrees well with observations both on timing and value.

The 2019 event shows a similar behavior (results available in the supporting material, S4 Fig). Air temperature in CTL follows quite closely the observations, although maximum daily temperatures are overestimated (as explained above). During the morning leading to the precipitation event, the model shows a rise of temperature to up to 30˚C a few hours before the observations, which we can attribute to clouds that are not simulated in CTL. As for dew point temperature, the model presents slight differences with the observations throughout the period. As for the 2018 event, a delay in the rise of dew point on the day of the event is present in CTL. The ability of the model to represent adequately air temperature and dew point indicates an overall good performance in capturing the surface processes.

3.1.2 Precipitation in the CTL experiment. The 2018 event is a large-scale system that crosses the Montreal Island and travels following the St-Laurent River from the southwest to the northeast. Two accumulation maxima are present in the CaPA analysis on both shores of the St-Laurence River (Fig 5E). The first maximum on the southeast shore of the river is well reproduced in the CTL experiment, with similar intensities and shape. The second maximum over the island of Montreal and on the northwest shore of the river is less intense in the model relative to the CaPA analysis. The model strongly underestimates this maximum, as if it was supressed completely, with less than 20 mm in the 24-hour accumulated precipitation on most of the grid points on the northwestern shore. On the other hand, a strong maximum in the southwest of the island is shown in the CTL results, which is absent in the CaPA analysis.

Hourly accumulations are available at a few stations in the area providing more details on the evolution of the rainfall event (Fig 5). Considering the system travelling from the southwest to the northeast, we accordingly choose four stations to investigate hourly rainfall intensities (see stations location in Fig 1) as follows: (a) a station upwind southwest of downtown (Sainte-Anne de Bellevue, WYQ), (b) a station in the downtown area (McTavish, WTA), (c) a station east of downtown (St-Hubert Airport, YHU) on the southeast shore of the river, and (d) a station downwind north of downtown (L'Assomption, WEW). Precipitation is simulated in the CTL experiment at around the same time as the observations, but intensities differ.

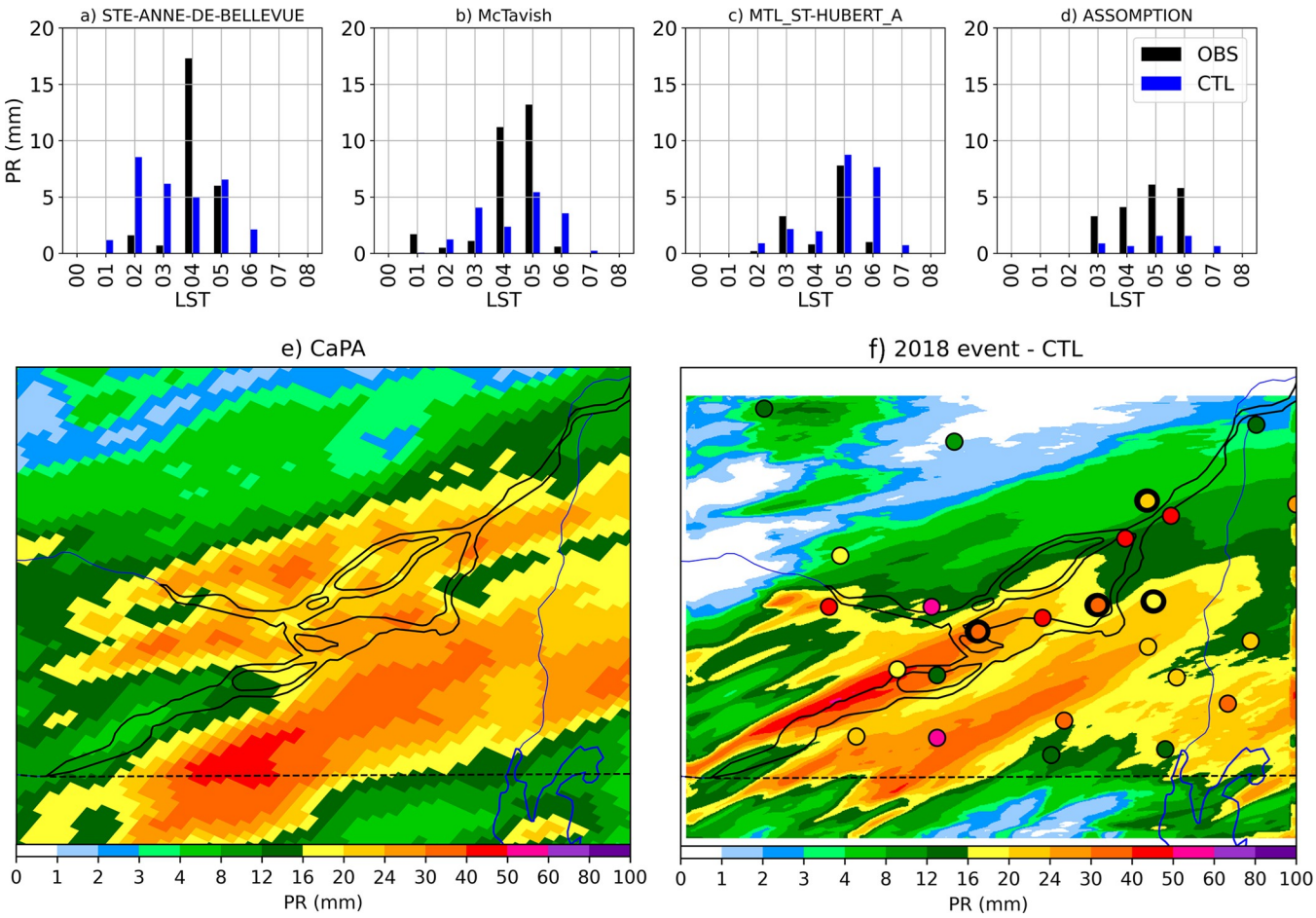

Fig 5. Observed and simulated rainfall for the 2018 event. a-d) Timeseries of 1h-precipitation accumulation in four different stations along the precipitation system: a) Ste Anne de Bellevue (up-wind of the city), b) McTavish (downtown), c) St-Hubert (suburb next to the downtown) and d) Assomption (down-wind). X-axis is the hour on July 17th 2018 (in local time). e-f) 24-h precipitation accumulation from 2018-07-16 2000 LST to 2018-08-17 2000 LST from e) CaPA analysis and f) CTL run (ensemble average), with colored circles representing observed accumulation values at available surface stations. The black arrow shows the global trajectory of the system. Made with Natural Earth (naturalearthdata.com), under the public domain license (https://creativecommons.org/publicdomain/).

https://doi.org/10.1371/journal.pclm.0000196.g005

Both the 24-h accumulations and the hourly precipitation seem to indicate a blockage of the precipitation system before crossing the city. Considering the split of the system on each shore of the river, the cell on the southeast shore is well represented in the model as shown at station YHU (Fig 5C), but the part passing over the city (defined by the path of stations WVQ, WTA and WEW) seemed blocked before crossing. The model simulates strong accumulations upwind (Fig 5A), consistent with observations, and very little rainfall over the city downtown (Fig 5B) and downwind (Fig 5D), underestimating accumulation in comparison to observations.

The 2019 event is a squall line that crosses perpendicularly the St-Laurence River and the island of Montreal during the afternoon from northwest to southeast (Fig 6E). The CaPA analysis shows a splitting of the squall line, where there are two poles of intense precipitation located on the northern and southwestern parts of the island, and lower intensity in the center (Fig 6E). The model simulates the squall line, with the same propagation direction and timing as the observed one (Fig 6), although convection over the city seem completely supressed. It splits into two smaller cells right before crossing the island, but contrary to the observations,

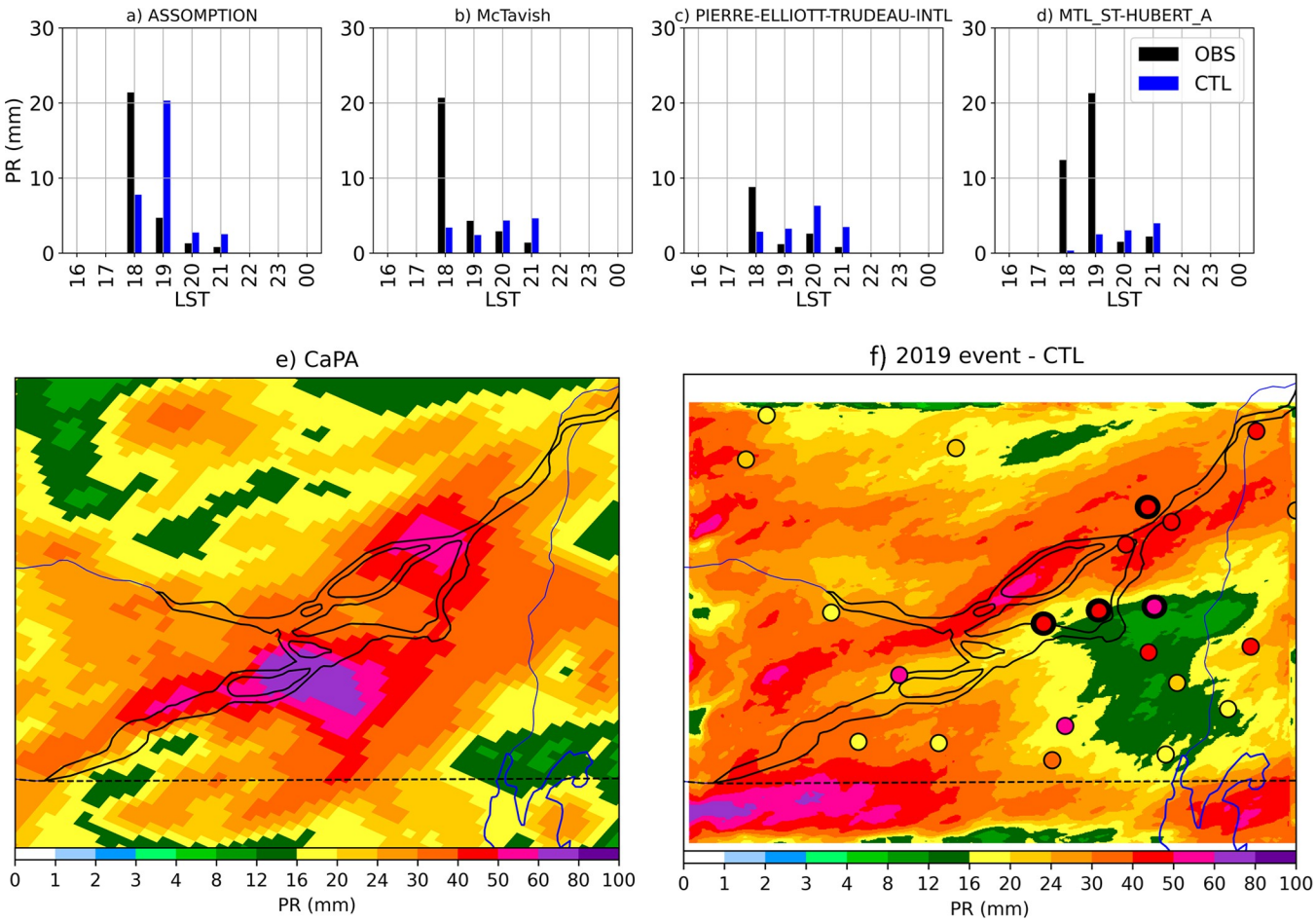

Fig 6. Observed and simulated rainfall for the 2019 event. a-d) Timeseries of 1h-precipitation accumulation in four different stations along the precipitation system: a) Assomption (up-wind of the city), b) McTavish (downtown), c) Pierre-Elliott-Trudeau (next to the downtown) and d) St-Hubert (down-wind). X-axis is the hour on July 11th 2019 (in local time). e-f) 24-h precipitation accumulation from 2019-07-11 0800 LST to 2019-07-12 0800 LST from e) CaPA analysis and f) CTL run (ensemble average), with colored circles representing observed accumulation values at available surface stations. The black arrow shows the global trajectory of the system. Made with Natural Earth (naturalearthdata.com), under the public domain license (https://creativecommons.org/publicdomain/).

https://doi.org/10.1371/journal.pclm.0000196.g006

both cells do not merge downwind of the city. This causes the dissipation of the squall line and therefore there is barely any precipitation downwind from the city (east and southeast of the Montreal island).

We choose four stations according to the propagation direction of the system to investigate hourly rainfall intensities as follows: (a) a station upwind (L'Assomption, WEW), (b) a station in the downtown area (McTavish, WTA), (c) a station southwest of downtown (Pierre-Elliott-Trudeau Airport, YUL), and (d) a station downwind east of downtown (St-Hubert Airport, YHU). At the stations upwind (WEW), downtown (WTA) and downwind (YHU), hourly observations show an intense peak of precipitation in the first two hours (20–30 mm) followed by a trail of less than 10 mm for the next two hours. The same signal is observed at the station YUL, but with lower hourly accumulations (less than 10 mm during the first hour). The model is consistent with observations upwind (Fig 5A), with about 30 mm accumulated rainfall in the first two hours, followed by traces of precipitation in the next two hours. As for the other three stations (Fig 5B, 5C and 5D), the model rather simulates a 4-hour period of constant rainfall (less than 5 mm/h), which indicates a dissipation of the squall line over the island of Montreal.

In both cases, the model seems to overestimate the blocking of the precipitation system before the city. In the 2018 event, accumulated precipitation indicated a blockage upwind and a possible bifurcation south of the city. In the 2019 event, the squall line seems to dissipate before crossing the river. In following sections, we will investigate whether this behavior is due to the presence of the city in the CTL experiment.

3.2 Effect on surface air temperature and humidity of mitigation scenarios

In this section, we investigate how the urban land-use/land-cover influences the surface air temperature, humidity and heat index, by either completely removing the urban area or by using heat mitigation scenarios.

3.2.1 NOURB versus CTL–surface. To quantify the impact of the city, we replace urban areas with vegetation in the NOURB experiment as described in section 2.3.2.

As expected, replacing all urban areas by vegetation significantly reduces surface air temperature (Fig 7A), with maximum differences up to 4–5˚C at night. Thermal properties of urban surfaces cause them to warm at faster rates than the surrounding rural areas during the day [41]. They are also more efficient than rural areas in storing heat, which is then released into the atmosphere during the night. This heat release increases the surface air temperature over urban surfaces, which explains such large temperature anomaly when they are removed in the NOURB experiment. Dew point, on the other hand, is up to 2–4˚C higher in the NOURB run than in the CTL run (Fig 7B), reaching maximum differences during the afternoon and at night. Such an increase is due to added water vapor from evapotranspiration.

The comfort felt by the city's inhabitants depends mostly on air temperature and humidity. A way to define this comfort is by calculating a heat index. The U.S. National Weather Service (NWS) algorithm is used in this study [48]. According to this algorithm, we find that heat index is decreased quite substantially in the NOURB experiment compared to the CTL experiment (Fig 7C). At night, there is an average decrease of heat index of 2–4˚C, with local peaks of up to 6˚C in the downtown area. During the day, the decrease of heat index is less noticeable, and it is around 1˚C.

The surface landscape and possible wind advection strongly determine the spatial pattern of the heat index, temperature, and humidity anomalies (Fig 8). Denser urban areas show a more substantial temperature and moisture differences than rural areas, as expected. Although these modifications are local, the hot and dry air is advected outside the city according to the wind's direction.

These results show how much the presence of a city like Montreal can modify the environmental properties of the city and surrounding areas, making it warmer and drier than the rural regions. The results for the July 2019 event are available in the supporting materials (S4 and S5 Fig). Intensities of differences between the NOURB and CTL are slightly lower for the 2019 event than the 2018 event. Maximum daily temperatures during the 2019 event (30˚C) are lower than during the 2018 event (32˚C), which indicates proportionality between the strength of the UHI and high temperatures. Our results also show the same diurnal pattern in both the 2018 and 2019 events, with the largest differences in heat index at night. Both events show similar advection patterns, however the signal is less clear in 2019 rather than during the 2018 event due to the surface wind that changes direction the day prior to the precipitation event.

3.2.2 ALB versus CTL–surface. In the ALB experiment only surface reflectivity is increased–the city's geometry, composition and materials are kept as in the CTL simulation, therefore thermal properties are not modified.

Surface air temperature is decreased throughout the whole day in the ALB experiment compared to the CTL experiment (Fig 7D), but to a lesser degree than in NOURB. As expected,

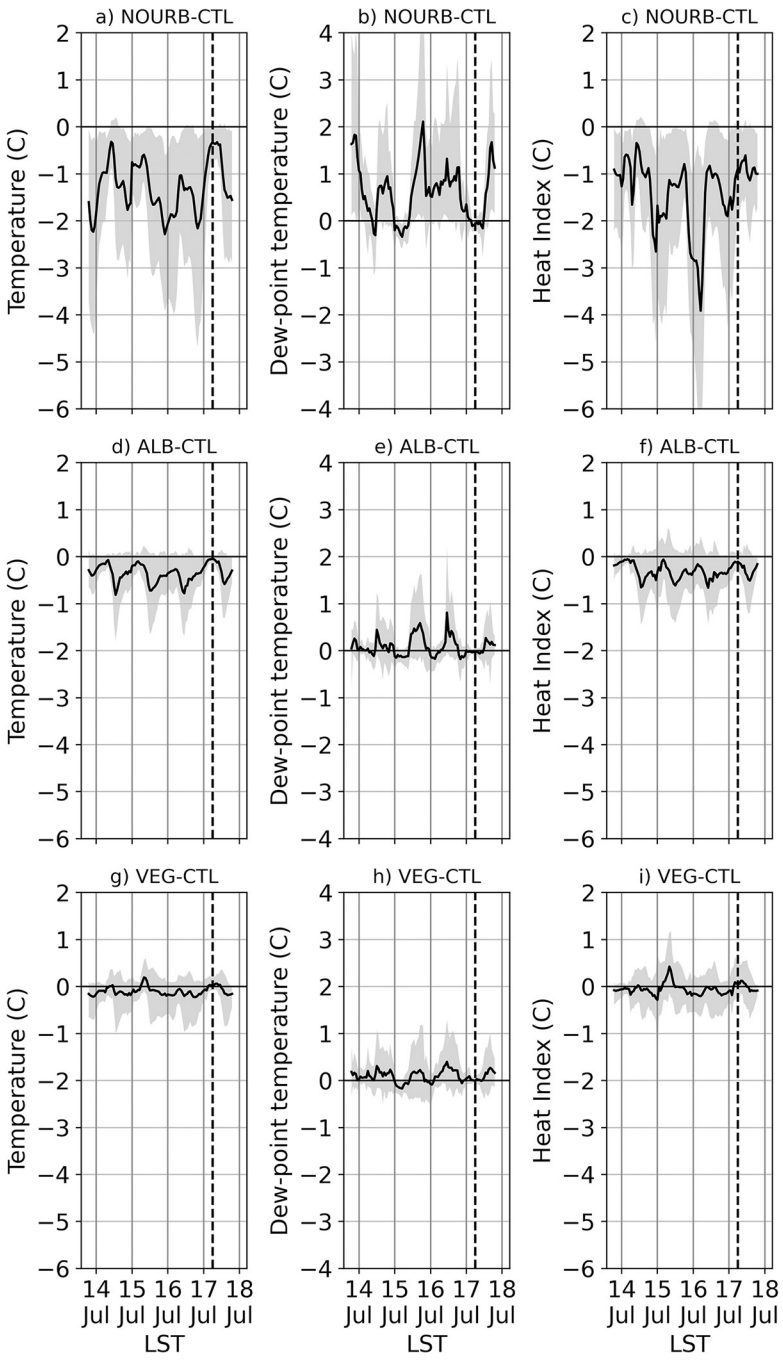

Fig 7. Changes in averaged 2-m air temperature, 2-m dew point and heat index for the 2018 event. Spatial timeseries of the difference in 2-m air temperature (a, d, g), 2-m dew point (b, e, h) and heat index (c, f, i) between NOURB-CTL (a, b, c), ALB-CTL (d, e, f) and VEG-CTL (g, h, i) model runs for the 2018 event. The black line is the spatial average on the island of Montreal of the difference between the sensitivity and the CTL experiments. The gray area is the 5th to 95th percentile and represents the spatial variability on the island of Montreal. Vertical lines show 00:00 local time. Made with Natural Earth (naturalearthdata.com), under the public domain license (https://creativecommons.org/publicdomain/).

https://doi.org/10.1371/journal.pclm.0000196.g007

this decrease is most important during the afternoon when the solar radiation is at its strongest. The higher albedo reflects more shortwave radiation in the ALB experiment; therefore, the lighter urban surface will warm less than the darker CTL surface. On the other hand, nighttime air temperatures in the ALB experiment are only slightly lower than in CTL (less than 0.5˚C). This is expected since emissivity and thermal properties of materials were not modified. The white and dark surfaces both release heat at night at similar rates; therefore, the nighttime UHI is not significantly affected by changes in albedo. The slight decrease in temperature can be associated with the fact that less heat is stored in the surfaces during the day.

The change in albedo slightly affects moisture (Fig 7E). Dew point is increased up to 1˚C during the afternoon in the ABL experiment compared to the CTL. Overall, the heat stress is lowered by the increased albedo (Fig 7F), which is in turn beneficial for the population living in the city.

3.2.3 VEG versus CTL–surface. In the VEG experiment, parts of the roads are replaced by low vegetation and the city's geometry is not modified compared to the CTL simulation. Considering the configuration used in the experiment, the weight attributed to the natural land cover fraction relative to the CTL will be more important in the VEG experiment; however, the natural land cover fraction is much less dominant in the VEG than in the NOURB experiment.

Vegetation has different properties than asphalt and cement roads, in particularly albedo, emissivity, soil moisture evolution through the day and presence of evapotranspiration. Therefore, air is cooler and moister over vegetation than over urban cover. Since the weight attributed to vegetation is larger in the VEG experiment than in the CTL, the overall results show a slight decrease in 2-m air temperature and a slight increase of dew point (Fig 7G and 7H). Some single grid points show the opposite behavior, especially in less dense areas, where the VEG experiment showed higher temperatures and lower dew point than the CTL experiment (S3A–S3C Fig). As those anomalies are isolated and located outside of the main urban core, the benefits of the scenario are still relevant.

These factors create a mixed effect on heat stress (Fig 7I), with areas that show a slight increase of comfort and others a slight decrease; in particular, an overall increase of comfort is simulated in dense urban areas (S3 Fig).

3.3 Effect on precipitation of mitigation scenarios

The results presented in section 3.2 indicate the clear impact of the urban land use on temperature and humidity at the surface. In this section, we investigate whether this modification of the surface layer properties (NOURB) can possibly affect rainfall.

3.3.1 2018 event. In terms of the effect of Montreal urban area on rainfall during July 2018 event, when the system passes through Montreal at night, our model experiment does not show any significant impact in terms of cumulative amount during 24 hours (Fig 9A). The small differences between NOURB and CTL are just random noise from the ensemble average. As mentioned in section 3.1.2, the CTL experiment shows less precipitation than observations over the city and downwind of the city, which we initially surmised to be related to the city's parametrisation in the model. However, replacing the urban surfaces and decreasing the roughness in the NOURB run does not seem to change the precipitation pattern. Therefore, the decreased rainfall over the city area in the CTL experiment cannot be due to the presence of built-up surfaces.

In addition, the surface instability caused by the UHI seems negligible in this case, as the rainfall event is part of a well-organized synoptic scale system. A vertical sounding of the modelled atmosphere in the CTL experiment at the start of the event shows very little convective available potential energy (CAPE) and a large zone of convective inhibition (CIN) at the

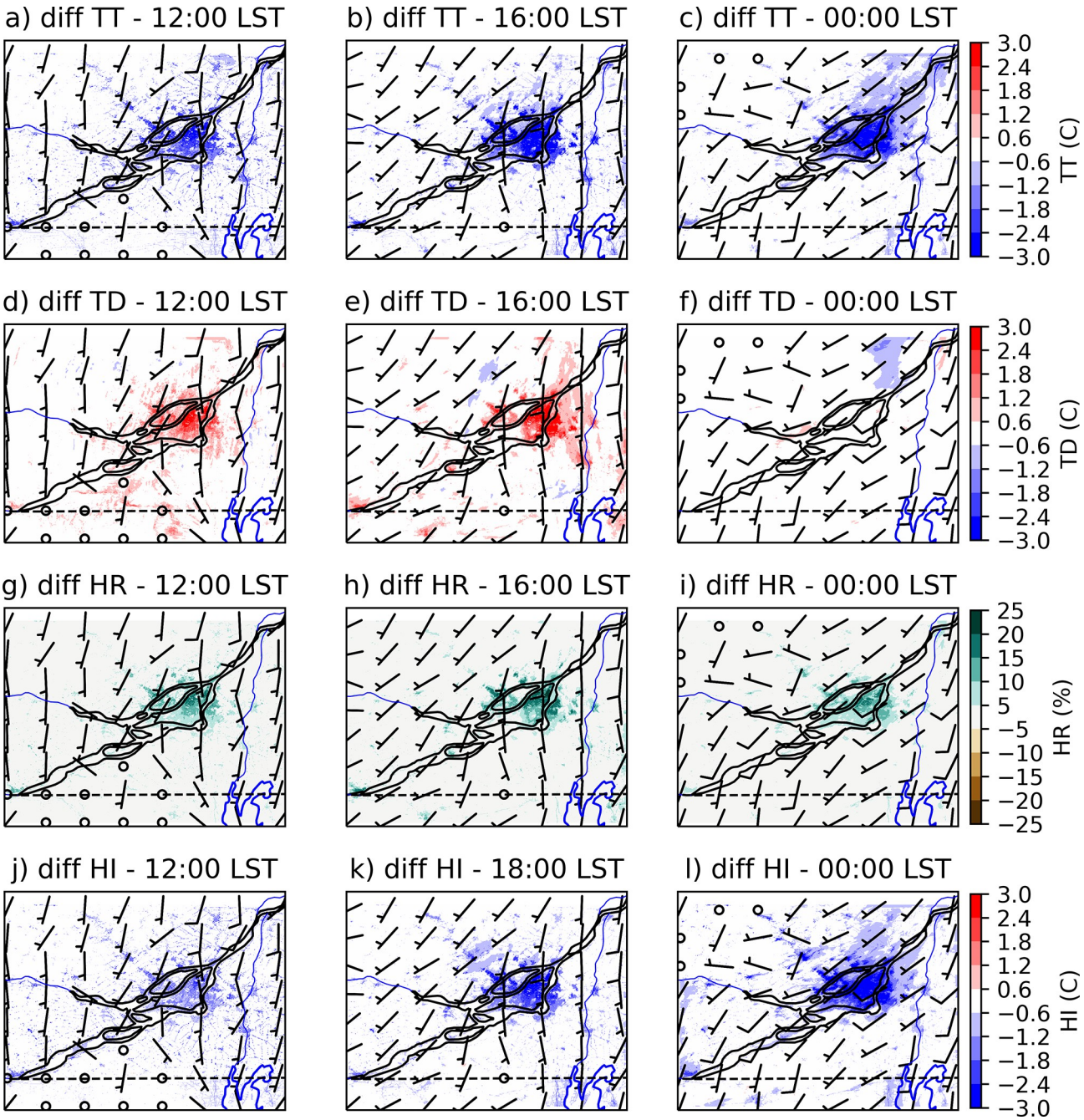

Fig 8. Changes in surface air temperature, dew point, relative humidity and heat index for the 2018 event. Anomalies in air temperature (a, b, c), dew-point temperature (d, e, f), relative humidity (g, h, i) and heat index (j, k, l) between NOURB and CTL experiments. The three columns correspond to different times: 2018-07-16 12:00 LST (left), 2018-07-16 18:00 LST (center) and 2018-07-17 00:00 LST (right). Surface winds for the CTL experiment are shown (in knots). Made with Natural Earth (naturalearthdata.com), under the public domain license (https://creativecommons.org/publicdomain/).

https://doi.org/10.1371/journal.pclm.0000196.g008

surface (Fig 10A), which indicates low atmospheric instability in the region. Modifying the land properties is expected to affect only the lower atmospheric levels, which is visible in the skew-T (Fig 10B). Hot and dry surface air in the CTL run generates a smaller surface CIN region compared to the NOURB run, but this reduction of CIN is not sufficient to provide a detectable impact on the system.

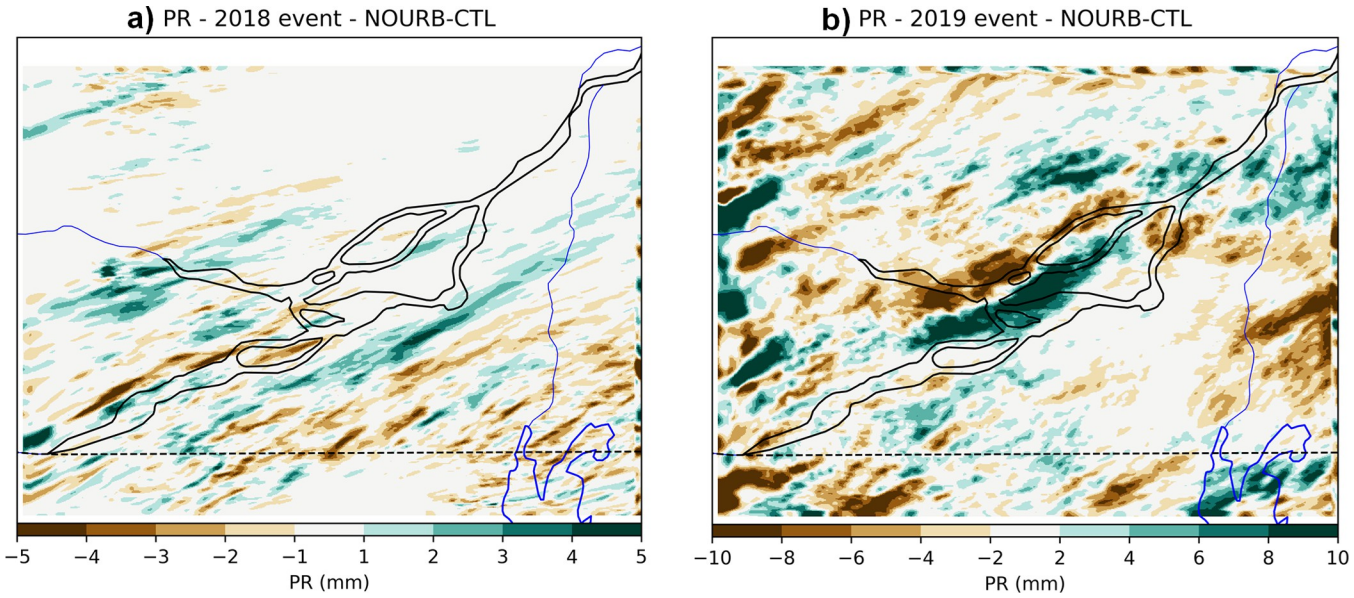

Fig 9. Changes in precipitation. Difference in accumulated precipitation between NOURB and CTL experiments for the 2018 event (a) and the 2019 event (b). Brown signifies more precipitation when the city is present. Made with Natural Earth (naturalearthdata.com), under the public domain license (https://creativecommons.org/publicdomain/).

https://doi.org/10.1371/journal.pclm.0000196.g009

3.3.2 2019 event. As opposed to the 2018 event, the July 2019 event is characterized by high instability. The front edge of the squall line is typically very unstable, with strong updrafts of moist air and the system travels over the city in the afternoon, when instability is at its maximum. Our results show a displacement of heavy rainfall towards the city in the NOURB simulation (Fig 9B) compared to the CTL experiment. Analysis of the composite reflectivity calculated by the model for the NOURB and CTL experiment shows no visible differences in timing and propagation of the squall line (Fig 11; the results at 1-km resolution are shown in order to see a larger portion of the squall line). In both cases, the system arrives at the city at 1900 local time with strong intensity. Accumulated rainfall differences between the NOURB and the CTL experiment show a signal at approximately the same location as the dissipation (over the city). There is a translation of accumulated rainfall of 10 mm more towards the island of Montreal in the NOURB experiment. In both cases, the squall line loses a lot on intensity downwind of the city, but it continues with the same propagation direction. This indicates that the presence of the city seems to affect the system on the upwind side of the island only.

The atmosphere is quite stable right before the passage of the squall line (Fig 10C and 10D). As the system passes over the island of Montreal, a large area of CAPE is present in the vertical sounding (Fig 10E and 10F). The CTL experiment (Fig 10E) shows a significantly larger CAPE area than the NOURB experiment (Fig 10F) which indicates that the presence of the city has more potential of enhancing convection. In our case, the squall line splits over the island of Montreal in both the CTL and NOURB experiments, which might explain why there is no significant effect on precipitation.

4 Discussion

Using a 250-m grid spacing for this type of study is interesting for many reasons. First, the surface heterogeneity is represented with very high accuracy and precision, therefore local processes of the urban heat island can be parametrized and resolved. A study from Leroyer et al.

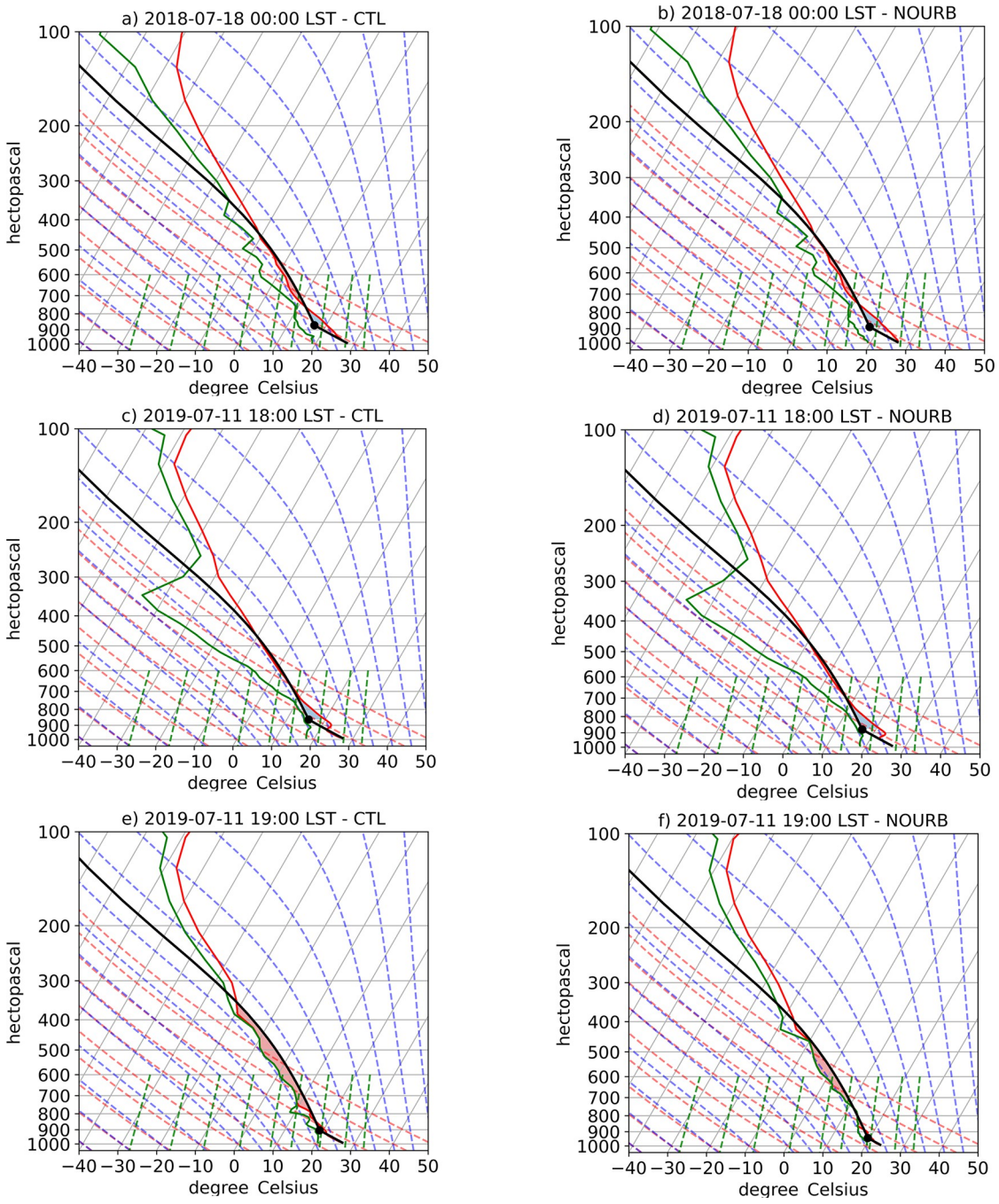

Fig 10. Skew-T diagram. Skew-T diagram on 2018-07-18 00:00 LST (a, b), 2019-07-11 18:00 LST (c, d) and 2019-07-11 19:00 LST (e, f) for the CTL experiment (left, a, c, e) and NOURB experiment (right, b, d, f) at the closest grid point to McTavish station. The red line is the temperature, the green line is the dew-point temperature and the black line is the air parcel lifted. The blue and red shaded areas represents the layers where convective inhibition (CIN) and convective available potential energy (CAPE) is present, respectively.

https://doi.org/10.1371/journal.pclm.0000196.g010

(2022) with a similar setup at 250-m horizontal resolution has proven better results than the 2.5-km operational analysis for 2-m temperature, dewpoint, winds and precipitation in summertime in Toronto (39). Precipitation patterns showed more details and have the potential to represent processes that cannot be resolved with the 2.5-km resolution (39). However, NWP

experiments at hectometric horizontal resolution are still experimental and further studies are necessary to strengthen their applicability.

4.1 Surface variables

The results presented in the study for 2-m temperature, dew point and thermal comfort agree with the existing literature. The NOURB experiment, in which all urban areas are replaced by low vegetation, highlights the intensity of the urban-induced modifications to local microclimate. The 2-m air temperature is greatly decreased especially at night, where differences with the CTL experiment reach 4–5˚C. The simulated anomalies are consistent with the difference in temperature between the urban station (McTavish, WTA) and the rural stations of Mirabel (YMX) to the west and Saint Hubert (YHU) to the east. Available observations show about the same maximum daily temperature between the urban station and the rural stations, but a 5˚C difference in minimum temperature. This decrease in temperature is well documented and the urban processes are well understood [5]. The added vegetation also has the effect of adding moisture in the air due to evapotranspiration, but, overall, the thermal comfort is improved in the NOURB experiment on average around 2–4˚C, and around 1˚C during the day on average. However, a notable spatial variability in the heat index anomalies is simulated over the island of Montreal, with larger differences over dense urban areas (4–6˚C) and negligible effects over existing large parks. Therefore, mitigating the effect of the UHI will lead to a remarkable increase in human comfort for the population living in the city.

In our study, we perform two mitigation scenarios, 1) increasing the urban surface's albedo (ALB) and 2) adding low vegetation at the street level (VEG). The increased albedo experiment shows a reduction of surface air temperature peaking during the afternoon, while nighttime temperature modification is negligible. According to literature, peak decrease of temperature due happens when sun radiation is maximal. At night, the air temperature is expected to be decreased in the ALB experiment compared to CTL, since there is less heating of the surface during the day [49]. Our results show this behavior, although the difference in temperature reaches almost zero as the end of the night. Our results show a slight increase of moisture during daytime in the ALB experiment, possibly due to an indirect effect on condensation. Overall, this strategy increases thermal comfort by 0.5–1˚C during the day. There are many ways to calculate the thermal comfort. In this study, the NWS heat index is used, which takes into consideration temperature and humidity. Other comfort indices also consider radiative exchanges at the street-level and winds, and studies have shown that increasing the ground-level albedo tend to decrease pedestrian comfort due to increased reflection [14,16,17]. No detailed analysis of the comfort was conducted as it is outside the scope of this study, therefore results on comfort changes for the ALB experiment must be interpreted carefully and are more representative of no-ground level albedo change. Further studies on the impact of mitigation scenarios on other comfort indices are necessary.

Adding low vegetation at the street level (VEG) in our numerical experiment shows a marginal and mixed impact on improving thermal comfort with slight reduced temperature and increased humidity. However, in dense urban areas, our results do show a decrease in temperature large enough to improve comfort. Adding trees instead of low vegetation would certainly have a more positive impact on thermal comfort since they interact directly with radiation by shading the surface [5]. This scenario was not considered, as such effect is not represented in our model. Investigation with other urban schemes in which the effect of trees is accounted for would provide better insights on mitigation strategies [50]. The results from the mitigation scenarios presented in this paper are in agreement with a similar study done for Montreal's local authorities [51] in which the effect of multiple mitigation scenarios is analyzed.

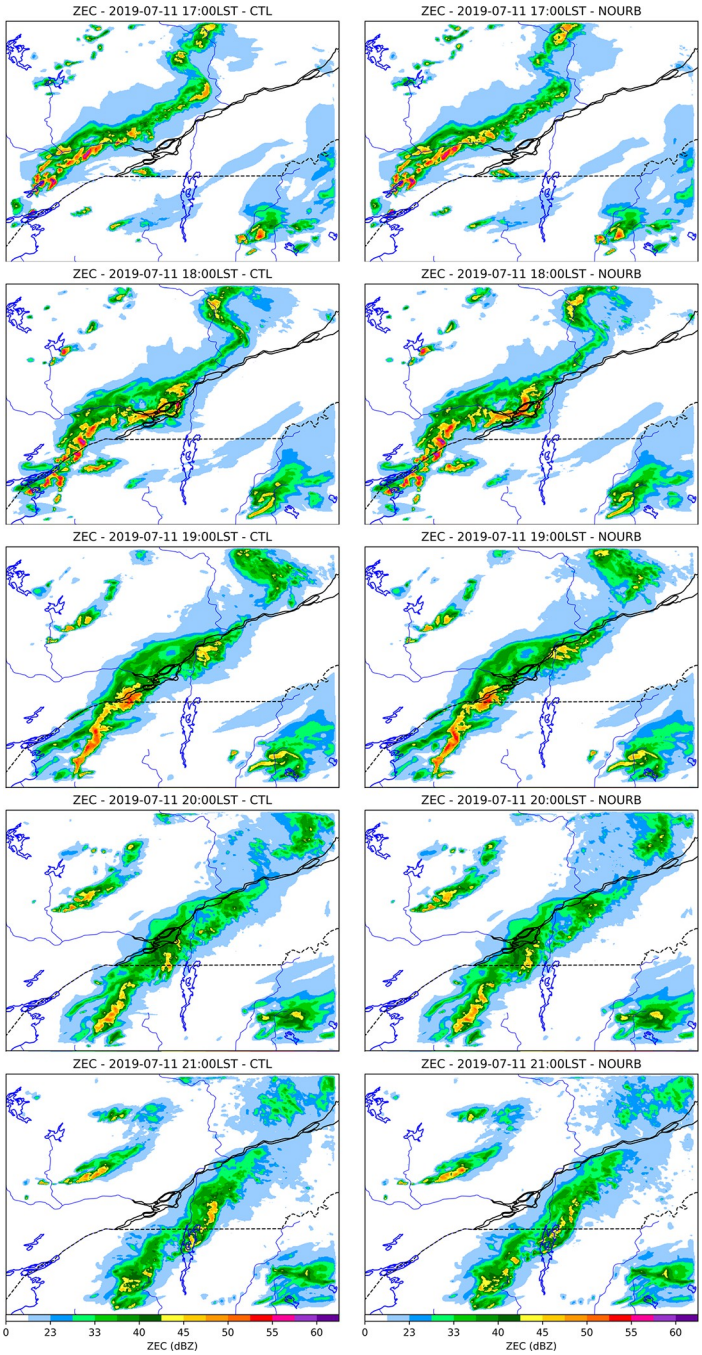

Fig 11. Model reflectivity for 2019 event. Maximum reflectivity at different times for the 2019 event for CTL (left) and NOURB (right) experiment. Times are, from top to bottom row, 1800, 1900, 2000, 2100 and 2200 LST on 2019-07-12. Made with Natural Earth (naturalearthdata.com), under the public domain license (https://creativecommons.org/publicdomain/).

https://doi.org/10.1371/journal.pclm.0000196.g011

Furthermore, Leroyer et al. [51] showed that the small reduction of air temperature ($< 0.5^{\circ}C$) associate with adding street-level vegetation could be greatly increased with forced soil irrigation (around $1^{\circ}C$). Hence, a combination of increased albedo and vegetation, would be greatly beneficial for the population living in dense urban areas.

4.2 Precipitation

For the 2018 event, in which an organized frontal system crossed the city at night, the impact on precipitation from the urban land use is not detected in our numerical experiments. The main reason is probably related to the fact that the UHI induced modification of the air mass above the city is not large enough to affect a large-scale organized system. These system's trajectories and intensity are defined by synoptic factors and a small perturbation at the surface has likely no impact. Furthermore, even if the signal of the UHI is strongest at night, the atmosphere is typically very stable, as compared to during the day, where the surface is very hot and generates substantial vertical instability. Nevertheless, Li et al. [20] have shown that in some cases, the UHI impacts on surface variables have a significant effect on atmospheric stability and hence, can enhance rainfall. For this reason, we investigate another event in 2019, characterized by large instability as a squall line develops in the afternoon and crosses Montreal from the northwest. In this case, the city seems to slightly affect the system. Results revealed more rainfall over the city in the CTL experiment compared to the NOURB case. The different spatial pattern of accumulated precipitation from the CTL and NOURB experiment shows a signal that indicates a possible impact from the land use: when the city is present the front seemed to be blocked before the island of Montreal before dissolving and there is slightly more precipitation over the island. The analysis of the vertical profile over the downtown area showed a large CAPE area at the time of the storm, which is significantly larger in the CTL experiment than NOURB. This indicates that the UHI can notably increase convection and instability, and therefore intensify the storm. However, in our experiment the squall line splits and weakens before passing over the city, which may explain why there is no significant differences on precipitation downwind of the city. Nevertheless, our results highlight how the presence of a large urban area can affect the vertical stability of the atmosphere, especially during periods of high instability.

Such impact on precipitation supports the finding of the above-mentioned study by Li et al. [20], suggesting an impact on rainfall of the UHI. However, our study indicates that conclusions on modification of precipitation due to urban land-use from isolated case studies have to be interpreted carefully as rainfall is highly variable and can be associated with different meteorological conditions. Therefore, other rainfall events, such as more localized events spurred by the instability created by the presence of the city itself should be considered to gain a more robust understanding of the city impacts on precipitation. Furthermore, a model intercomparison and further investigation on the model configuration and the schemes used for the representation of physical processes at the surface and in the boundary layer could help shedding light on model inaccuracy and misrepresentation of the rainfall systems.

5 Conclusion

The objective of this study is to determine potential effects of the city of Montreal and the impact of different urban development strategies on the local climate. At present, studies have investigated the UHI in Montreal [24,25] and the possible impact of mitigation scenarios [51]; however, little is known on the UHI impact on summer rainfall. Numerical experiments with a subkilometer (250 m) Numerical Weather Prediction System using GEM as atmospheric model and TEB as surface scheme are performed, following recent configurations used for urban studies at ECCC [39].

Local surface climate is in general well represented by our numerical model. Overall, air temperature and dew-point temperature followed accurately the observations available for the studied periods with some minor discrepancies. As for precipitation, the model was able to simulate the rainfall event for both the 2018 and the 2019 events, although presented

differences with the observations. In both cases, accumulated precipitation was lower over and downwind of the city, suggesting a possible blockage of the systems by the city.

Finally, Montreal has a particular geographical setting since it is an island in a valley and it is known that storms have the tendency to bifurcate or split around Montreal. This might be attributed to the river that modifies low-level divergence, protecting the island from strong storms [52]. The 2018 event did not show this behavior, but the model simulated a bifurcation of the system in all experiments. Observations as well as the experiments of the 2019 event showed a split of the squall line, although the model misses the merge of the system over the city. It may well be that our model overestimates the processes that influence the bifurcation and split. Additional studies of model sensitivity to the river properties (temperature and presence) and for other heavy rain events are necessary to shed light on the role of Montreal island in bifurcating or splitting storms.

Supporting information

S1 Fig. Driving data ensemble. The 9-member ensemble driving data from the 2.5-km HRDPS forecast. The 2019 event uses a 6-member ensemble.
(TIF)

S2 Fig. Changes in surface air temperature, dew point, relative humidity and heat index between ALB and CTL for the 2018 event. Same as Fig 8, but for the ALB experiment. Anomalies in air temperature (a, b, c), dew-point temperature (d, e, f), relative humidity (g, h, i) and heat index (j, k, l) between ALB and CTL experiments. The three columns correspond to different times: 2018-07-16 12:00 LST (left), 2018-07-16 18:00 LST (center) and 2018-07-17 00:00 LST (right). Surface winds for the CTL experiment are shown (in knots). Made with Natural Earth (naturalearthdata.com), under the public domain license (https://creativecommons.org/publicdomain/).
(TIF)

S3 Fig. Same as S2 Fig, but for the VEG experiment. Made with Natural Earth (naturalearthdata.com), under the public domain license (https://creativecommons.org/publicdomain/).
(TIF)

S4 Fig. Timeseries of observed and simulated surface variables for the 2019 event. Same as Fig 4, but for the 2019 event. Observed (black) and simulated (blue) surface air temperature (TT, a and b) and dew point temperature (TD, c and d) at station McTavish (WTA, a and c) and St-Hubert (YHU, b and d) for the 2018 event. The blue shading shows the ensemble spread.
(TIF)

S5 Fig. Changes in averaged surface air temperature, relative humidity and heat index for the 2019 event. Spatial timeseries of the difference in surface air temperature (a), relative humidity (b) and heat index (c) between NOURB-CTL model runs for the 2019 event. The black line is the spatial average on the island of Montreal of the difference between the sensitivity and the CTL experiments. The gray area is the 5th to 95th percentile and represents the spatial variability on the island of Montreal. Vertical lines show 00:00 local time.
(TIF)

S6 Fig. Changes in surface air temperature, dew point, relative humidity and heat index between NOURB and CTL for the 2019 event. Same as Fig 8, but for the 2019 event. Anomalies in air temperature (a, b, c), dew-point temperature (d, e, f), relative humidity (g, h, i) and heat index (j, k, l) between NOURB and CTL experiments. The three columns correspond to

different times: 2019-07-11 08:00 LST (left), 2019-07-11 12:00 LST (center) and 2019-07-11 18:00 LST (right). Surface winds for the CTL experiment are shown (in knots). Made with Natural Earth (naturalearthdata.com), under the public domain license (https://creativecommons.org/publicdomain/).
(TIF)

S1 Table. Weather stations. Information and localisation of weather stations used as observations.
(DOCX)

Author Contributions

Conceptualization: Audrey Lauer, Francesco S. R. Pausata, Sylvie Leroyer, Daniel Argueso.

Data curation: Audrey Lauer.

Investigation: Audrey Lauer.

Methodology: Sylvie Leroyer.

Project administration: Francesco S. R. Pausata.

Resources: Sylvie Leroyer.

Software: Audrey Lauer.

Validation: Audrey Lauer.

Visualization: Audrey Lauer.

Writing – original draft: Audrey Lauer, Francesco S. R. Pausata, Sylvie Leroyer, Daniel Argueso.

Writing – review & editing: Audrey Lauer, Francesco S. R. Pausata, Sylvie Leroyer.

References

1. World urbanization prospects: the 2018 revision. New York: United Nations; 2019.
2. Mills G. Luke Howard and The Climate of London. Weather. 2008 Jun; 63(6):153–7.
3. Oke TR. The energetic basis of the urban heat island. Q J R Meteorol Soc. 1982; 108(455):1–24.
4. Stewart ID. Redifining the urban heat island [Thesis]. [Vancouver]: University of British Columbia; 2011.
5. Oke TR, Mills G, Christen A, Voogt JA. Urban Climates. Cambridge University Press; 2017. 549 p.
6. He BJ, Ding L, Prasad D. Wind-sensitive urban planning and design: Precinct ventilation performance and its potential for local warming mitigation in an open midrise gridiron precinct. J Build Eng. 2020 May; 29:101145.
7. Krayenhoff ES, Jiang T, Christen A, Martilli A, Oke TR, Bailey BN, et al. A multi-layer urban canopy meteorological model with trees (BEP-Tree): Street tree impacts on pedestrian-level climate. Urban Clim. 2020 Jun 1; 32:100590.
8. Lee H, Mayer H, Chen L. Contribution of trees and grasslands to the mitigation of human heat stress in a residential district of Freiburg, Southwest Germany. Landsc Urban Plan. 2016 Apr 1; 148:37–50.
9. Berardi U, Jandaghian Z, Graham J. Effects of greenery enhancements for the resilience to heat waves: A comparison of analysis performed through mesoscale (WRF) and microscale (Envi-met) modeling. Sci Total Environ. 2020 Dec 10; 747:141300. https://doi.org/10.1016/j.scitotenv.2020.141300 PMID: 32791415
10. Yang J, Wang ZH, Kaloush KE, Dylla H. Effect of pavement thermal properties on mitigating urban heat islands: A multi-scale modeling case study in Phoenix. Build Environ. 2016 Nov 1; 108:110–21.
11. Yang F, Lau SSY, Qian F. Thermal comfort effects of urban design strategies in high-rise urban environments in a sub-tropical climate. Archit Sci Rev. 2011 Nov; 54(4):285–304.

12. Taha H, Akbari H, Rosenfeld A, Huang J. Residential cooling loads and the urban heat island—the effects of albedo. Build Environ. 1988 Jan 1; 23(4):271–83.

13. Krayenhoff ES, Voogt JA. Impacts of Urban Albedo Increase on Local Air Temperature at Daily–Annual Time Scales: Model Results and Synthesis of Previous Work. J Appl Meteorol Climatol. 2010 Aug 1; 49 (8):1634–48.

14. Taleghani M, Berardi U. The effect of pavement characteristics on pedestrians' thermal comfort in Toronto. Urban Clim. 2018 Jun 1; 24:449–59.

15. Broadbent AM, Coutts AM, Tapper NJ, Demuzere M. The cooling effect of irrigation on urban microclimate during heatwave conditions. Urban Clim. 2018 Mar 1; 23:309–29.

16. Erell E, Pearlmutter D, Boneh D, Kutiel PB. Effect of high-albedo materials on pedestrian heat stress in urban street canyons. Urban Clim. 2014 Dec; 10:367–86.

17. Herrmann J, Matzarakis A. Mean radiant temperature in idealised urban canyons—examples from Freiburg, Germany. Int J Biometeorol. 2012 Jan; 56(1):199–203. https://doi.org/10.1007/s00484-010-0394-1 PMID: 21221656

18. Liu J, Niyogi D. Meta-analysis of urbanization impact on rainfall modification. Sci Rep. 2019 May 13; 9 (1):7301. https://doi.org/10.1038/s41598-019-42494-2 PMID: 31086196

19. Bornstein R, Lin Q. Urban heat islands and summertime convective thunderstorms in Atlanta: three case studies. Atmos Environ. 2000 Feb 1; 34(3):507–16.

20. Li Y, Fowler HJ, Argüeso D, Blenkinsop S, Evans JP, Lenderink G, et al. Strong Intensification of Hourly Rainfall Extremes by Urbanization. Geophys Res Lett [Internet]. 2020 Jul 28 [cited 2022 Dec 11]; 47 (14). Available from: https://onlinelibrary.wiley.com/doi/10.1029/2020GL088758

21. Zhang Y, Miao S, Dai Y, Bornstein R. Numerical simulation of urban land surface effects on summer convective rainfall under different UHI intensity in Beijing: Urban Effects on Rainfall in Beijing. J Geophys Res Atmospheres. 2017 Aug 16; 122(15):7851–68.

22. Shepherd JM. Impacts of urbanization on precipitation and storms: Physical insights and vulnerabilities. Clim Vulnerability. 2013; 5:109–25.

23. Niyogi D, Pyle P, Lei M, Arya SP, Kishtawal CM, Shepherd M, et al. Urban Modification of Thunderstorms: An Observational Storm Climatology and Model Case Study for the Indianapolis Urban Region. J Appl Meteorol Climatol. 2011 May 1; 50(5):1129–44.

24. Oke TR, Maxwell GB. Urban heat island dynamics in Montreal and Vancouver. Atmospheric Environ 1967. 1975; 9(2):191–200.

25. Wang Y, Akbari H. The effects of street tree planting on Urban Heat Island mitigation in Montreal. Sustain Cities Soc. 2016 Nov 1; 27:122–8.

26. Teufel B, Sushama L, Huziy O, Diro GT, Jeong DI, Winger K, et al. Investigation of the mechanisms leading to the 2017 Montreal flood. Clim Dyn. 2019 Apr 1; 52(7):4193–206.

27. Madsen H, Lawrence D, Lang M, Martinkova M, Kjeldsen TR. Review of trend analysis and climate change projections of extreme precipitation and floods in Europe. J Hydrol. 2014 Nov; 519:3634–50.

28. Huong HTL, Pathirana A. Urbanization and climate change impacts on future urban flooding in Can Tho city, Vietnam. Hydrol Earth Syst Sci. 2013 Jan 29; 17(1):379–94.

29. Trenberth KE. Changes in precipitation with climate change. Clim Res. 2011 Mar 31; 47(1–2):123–38.

30. Miller JD, Hutchins M. The impacts of urbanisation and climate change on urban flooding and urban water quality: A review of the evidence concerning the United Kingdom. J Hydrol Reg Stud. 2017 Aug; 12:345–62.

31. Kundzewicz ZW, Pińskwar I, Brakenridge GR. Large floods in Europe, 1985–2009. Hydrol Sci J. 2013 Jan; 58(1):1–7.

32. Côté J, Gravel S, Méthot A, Patoine A, Roch M, Staniforth A. The Operational CMC–MRB Global Environmental Multiscale (GEM) Model. Part I: Design Considerations and Formulation. Mon Weather Rev. 1998 Jun 1; 126(6):1373–95.

33. Husain SZ, Girard C. Impact of Consistent Semi-Lagrangian Trajectory Calculations on Numerical Weather Prediction Performance. Mon Weather Rev. 2017 Oct 1; 145(10):4127–50.

34. Noilhan J, Planton S. A Simple Parameterization of Land Surface Processes for Meteorological Models. Mon Weather Rev. 1989 Mar 1; 117(3):536–49.

35. Bélair S, Crevier LP, Mailhot J, Bilodeau B, Delage Y. Operational Implementation of the ISBA Land Surface Scheme in the Canadian Regional Weather Forecast Model. Part I: Warm Season Results. J Hydrometeorol. 2003 Apr 1; 4(2):352–70.

36. Masson V. A Physically-Based Scheme For The Urban Energy Budget In Atmospheric Models. Bound-Layer Meteorol. 2000 Mar 1; 94(3):357–97.

37. Lemonsu A, Belair S, Mailhot J. The New Canadian Urban Modelling System: Evaluation for Two Cases from the Joint Urban 2003 Oklahoma City Experiment. Bound-Layer Meteorol. 2009 Oct 1; 133 (1):47–70.

38. Oke TR. Canyon geometry and the nocturnal urban heat island: Comparison of scale model and field observations. J Climatol. 1981 Jul; 1(3):237–54.

39. Leroyer S, Bélair S, Souvanlasy V, Vallée M, Pellerin S, Sills D. Summertime Assessment of an Urban-Scale Numerical Weather Prediction System for Toronto. Atmosphere. 2022 Jul; 13(7):1030.

40. Macdonald RW, Griffiths RF, Hall DJ. An improved method for the estimation of surface roughness of obstacle arrays. Atmos Environ. 1998 Jun; 32(11):1857–64.

41. Bélair S, Mailhot J, Girard C, Vaillancourt P. Boundary Layer and Shallow Cumulus Clouds in a Medium-Range Forecast of a Large-Scale Weather System. Mon Weather Rev. 2005 Jul 1; 133 (7):1938–60.

42. Milbrandt JA, Yau MK. A Multimoment Bulk Microphysics Parameterization. Part I: Analysis of the Role of the Spectral Shape Parameter. J Atmospheric Sci. 2005 Sep 1; 62(9):3051–64.

43. Bélair S, Leroyer S, Seino N, Spacek L, Souvanlassy V, Paquin-Ricard D. Role and Impact of the Urban Environment in a Numerical Forecast of an Intense Summertime Precipitation Event over Tokyo. 気象集誌 第2輯. 2018;advpub:2018–011.

44. Honnert R, Efstathiou GA, Beare RJ, Ito J, Lock A, Neggers R, et al. The Atmospheric Boundary Layer and the "Gray Zone" of Turbulence: A Critical Review. J Geophys Res Atmospheres [Internet]. 2020 Jul 16 [cited 2023 Mar 9]; 125(13). Available from: https://onlinelibrary.wiley.com/doi/10.1029/2019JD030317

45. Mason PJ, Brown AR. On Subgrid Models and Filter Operations in Large Eddy Simulations. J Atmospheric Sci. 1999 Jul; 56(13):2101–14.

46. Fortin V, Roy G, Stadnyk T, Koenig K, Gasset N, Mahidjiba A. Ten Years of Science Based on the Canadian Precipitation Analysis: A CaPA System Overview and Literature Review. Atmosphere-Ocean. 2018 May 27; 56(3):178–96.

47. World Meteorological Organization (WMO). Guide to Instruments and Methods of Observation (WMO-No. 8). 2018th and 2021 editions ed. Geneva: WMO; 2018. 224 p. (WMO).

48. Anderson GB, Bell ML, Peng RD. Methods to Calculate the Heat Index as an Exposure Metric in Environmental Health Research. Environ Health Perspect. 2013 Oct; 121(10):1111–9. https://doi.org/10.1289/ehp.1206273 PMID: 23934704

49. Lynn BH, Carlson TN, Rosenzweig C, Goldberg R, Druyan L, Cox J, et al. A Modification to the NOAH LSM to Simulate Heat Mitigation Strategies in the New York City Metropolitan Area. J Appl Meteorol Climatol. 2009 Feb 1; 48(2):199–216.

50. Redon EC, Lemonsu A, Masson V, Morille B, Musy M. Implementation of street trees within the solar radiative exchange parameterization of TEB in SURFEX v8.0. Geosci Model Dev. 2017 Jan 25; 10 (1):385–411.

51. Leroyer S, Bélair S, Alavi N, Munoz-Alpizar R, Nikiema O, Popadic I. Influence des aménagements du tissu urbain sur la micro-météorologie et le confort thermique: Cas des villes de Montréal et Toronto [Internet]. Zenodo; 2019 Sep [cited 2022 Dec 11]. Available from: https://zenodo.org/record/7324545.

52. Ouellette-Vézina H. Orages violents: La province victime d'un. . . derecho. La Presse [Internet]. 2022 May 24 [cited 2022 Dec 11]; Available from: https://www.lapresse.ca/actualites/2022-05-24/orages-violents/la-province-victime-d-un-derecho.php.